N_2O and CH_4 variations during the last glacial epoch: Insight into global processes

Jacqueline Flückiger,[1] Thomas Blunier,[1] Bernhard Stauffer,[1] Jérôme Chappellaz,[2] Renato Spahni,[1] Kenji Kawamura,[1] Jakob Schwander,[1] Thomas F. Stocker,[1] and Dorthe Dahl-Jensen[3]

Received 10 July 2003; revised 9 December 2003; accepted 12 December 2003; published 30 January 2004.

[1] Greenhouse gas measurements along polar ice cores provide important insight into the former composition of the atmosphere, its natural variations, and the responses to fast climatic changes in the past. We present high-resolution nitrous oxide (N_2O) and methane (CH_4) records measured along two ice cores from central Greenland covering part of Marine Isotope Stages 3 and 4 in the last glacial epoch. The N_2O data confirm the hypothesis that N_2O shows variations in phase to fast climatic changes observed in the Northern Hemisphere, the so-called Dansgaard-Oeschger (D-O) events. Variations exist not only for events with a long duration (1500 years and more) but also for the shorter ones. The comparison with CH_4 unveils interesting differences between the response of CH_4 and N_2O to D-O events. While the average amplitudes of CH_4 oscillations associated with D-O events are similar to those of the Northern Hemisphere summer insolation, the magnitude of the N_2O concentration change instead correlates with the duration of the D-O events. The records give further insight into the timing of concentration changes at the beginning of D-O events. They show that for long-lasting events the N_2O concentration starts to increase before both the sharp increase in the CH_4 concentration and the temperature reconstructed for Greenland. *INDEX TERMS:* 0325 Atmospheric Composition and Structure: Evolution of the atmosphere; 0315 Atmospheric Composition and Structure: Biosphere/atmosphere interactions; 1827 Hydrology: Glaciology (1863); 3344 Meteorology and Atmospheric Dynamics: Paleoclimatology; *KEYWORDS:* CH_4, last glacial epoch, N_2O

Citation: Flückiger, J., T. Blunier, B. Stauffer, J. Chappellaz, R. Spahni, K. Kawamura, J. Schwander, T. F. Stocker, and D. Dahl-Jensen (2004), N_2O and CH_4 variations during the last glacial epoch: Insight into global processes, *Global Biogeochem. Cycles*, *18*, GB1020, doi:10.1029/2003GB002122.

1. Introduction

[2] Methane (CH_4) and nitrous oxide (N_2O) are the most important greenhouse gases after water vapor and carbon dioxide (CO_2). In the past, they all underwent significant variations on glacial-interglacial timescales [*Flückiger et al.*, 1999; *Petit et al.*, 1999] as well as on millennial timescales during the last glacial epoch [*Flückiger et al.*, 1999; *Indermühle et al.*, 2000; *Blunier and Brook*, 2001; *Sowers et al.*, 2003]. N_2O and CH_4 variations in the last glacial period show a close relation to the fast climatic changes in the Northern Hemisphere, the so-called Dansgaard-Oeschger (D-O) events (Figure 1). This is in contrast to the CO_2 concentration, which shows variations rather in phase with the temperature reconstructed for Antarctica. The origin of these concentration variations is thought to be caused mainly by variations in the different sources of the greenhouse gases, which are the ocean for CO_2, wetlands for CH_4, and for N_2O terrestrial soils (about two thirds of the total source in preanthropogenic times) as well as the ocean (about one third of the total source in preanthropogenic times).

[3] Understanding the causes, mechanisms, and potential feedbacks of fast climatic changes in the past is of great interest for a better understanding of the climate system. High-resolution N_2O and CH_4 records can provide such insight as well as important information about global biogeochemical cycles. Variations of the N_2O and the CH_4 concentration in the past had only a minor effect on the direct greenhouse effect. However, knowledge about the natural variability of greenhouse gas concentrations and their relation to fast climatic changes is also of interest in terms of present climate change. Over the last 250 years, atmospheric N_2O, CH_4, and CO_2 contents have increased dramatically mainly due to anthropogenic emissions (see *Stauffer et al.* [2002] for an overview). By 1998, respective levels had reached global means of 314 parts per billion by volume (ppbv), 1745 ppbv [*Intergovernmental Panel on*

[1]Climate and Environmental Physics, Physics Institute, University of Bern, Bern, Switzerland.
[2]CNRS Laboratoire de Glaciologie et Géophysique de l'Environnement (LGGE), Grenoble, France.
[3]Niels Bohr Institute, Department of Geophysics, University of Copenhagen, Copenhagen, Denmark.

0886-6236/04/2003GB002122$12.00

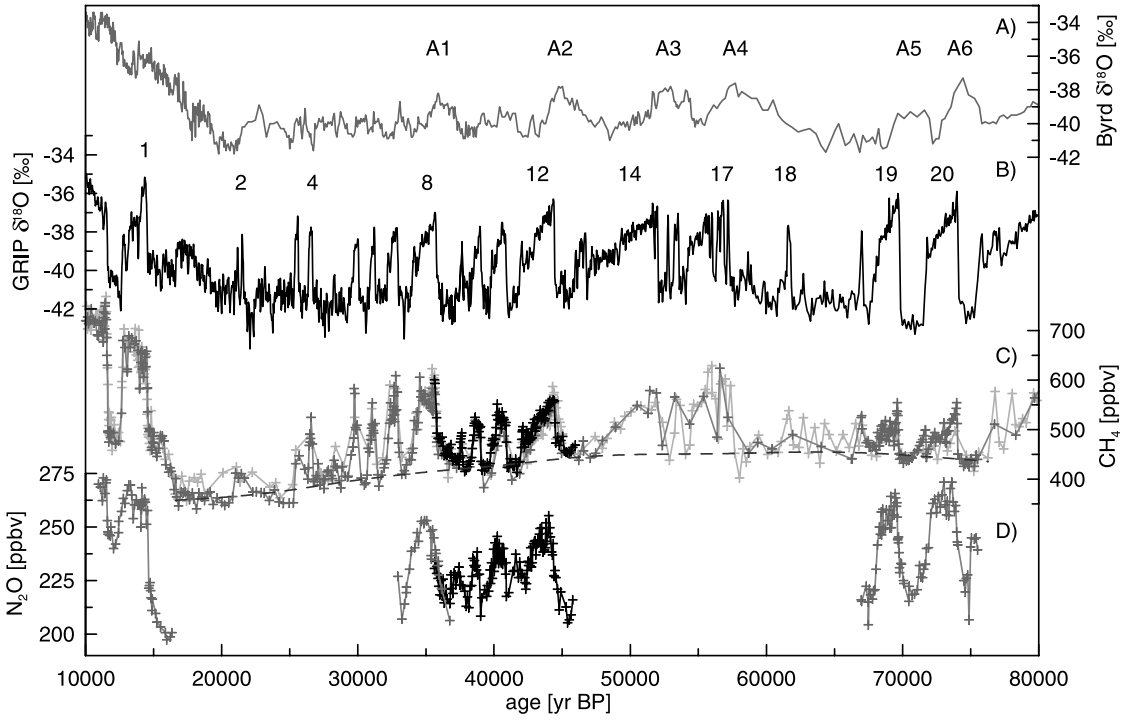

Figure 1. Isotopic, CH_4, and N_2O data from Greenland and Antarctica over the last glacial epoch and the transition to the Holocene on the GRIP SS09 timescale [*Johnsen et al.*, 1995; *Schwander et al.*, 1997; *Blunier and Brook*, 2001]. (a) The $\delta^{18}O$ of ice from Byrd station, West Antarctica [*Johnsen et al.*, 1972]. (b) The $\delta^{18}O$ of ice from GRIP, Central Greenland [*Dansgaard et al.*, 1993]. The numbers of the D-O events are given according to *Dansgaard et al.* [1993]. (c) CH_4 data from NGRIP (black), GRIP (dark shading) (*Dällenbach et al.* [2000], *Blunier and Brook* [2001], and this study), and GISP2 (light shading) [*Brook et al.*, 1999; *Blunier and Brook*, 2001]. The long-term variations in the CH_4 baseline are highlighted by the dashed line. It was calculated with the method developed for excluding N_2O artifacts (see Appendix A), using a cutoff period of 20 kyr and an offset value of 15 ppbv. (d) N_2O data from NGRIP (black) and GRIP (shaded) (*Flückiger et al.* [1999] and this study). N_2O artifacts were excluded for this figure.

Climate Change (*IPCC*), 2001], and 367 parts per million by volume (ppmv) [*Keeling and Whorf*, 2000]. Ongoing global warming could enhance future greenhouse gas emissions from natural sources.

2. Method and Data Evaluation

2.1. Method

[4] Samples of about 40 g of polar ice are used at Bern for the CH_4 and N_2O measurements. The air trapped in the ice is extracted with a melt-refreezing method, and the extracted gas is then analyzed for $N_2 + O_2 + Ar$, N_2O, and CH_4 by gas chromatography [*Chappellaz et al.*, 1997; *Flückiger et al.*, 2002]. Tests with bubble-free ice (air-free ice produced by a repeatedly applied zone melting technique starting with highly purified water) and two standard gases (201 ppbv N_2O/408 CH_4, 304 ppbv N_2O/1050 ppbv CH_4) have shown that the melt-refreezing extraction developed for CH_4 can be used for N_2O despite the high solubility of N_2O in water. However, the extraction causes a loss of $(2.32 \pm 0.47) \times 10^{-8}$ mL of N_2O (at standard temperature and pressure) corresponding to a correction of about 6 ± 1.2 ppbv with a typical sample size of 40 g of ice. The given analytical uncertainty σ of the N_2O results is a combination ($\sigma^2 = \sigma_e^2 + \sigma_d^2$) of the uncertainty from the extraction process σ_e, which is determined by measuring bubble-free ice samples with standard gas, and the actual precision of the detectors σ_d. The latter is taken into account by the scatter of three individual measurements per extracted ice core sample multiplied by the corresponding t-value of the t-distribution due to the small number of injections. The mean analytical uncertainty (1σ) for the N_2O data presented in this study is 3.7 ppbv. The reproducibility of neighboring ice samples from artifact-free ice like the Holocene part of the Dome C ice core [*Flückiger et al.*, 2002] is within this analytical uncertainty. For CH_4 the analytical uncertainty (1σ) has been estimated at 10 ppbv [*Chappellaz et al.*, 1997]. Further details about the method, the tests performed, and the calibration of the standard gases used are given by *Flückiger et al.* [2002] and *Chappellaz et al.* [1997].

[5] Here we present high-resolution records of CH_4 and N_2O covering two time periods in Marine Isotope Stage (MIS) 3 and 4 in the last glacial epoch. Measurements were performed along the North Greenland Ice Core Project

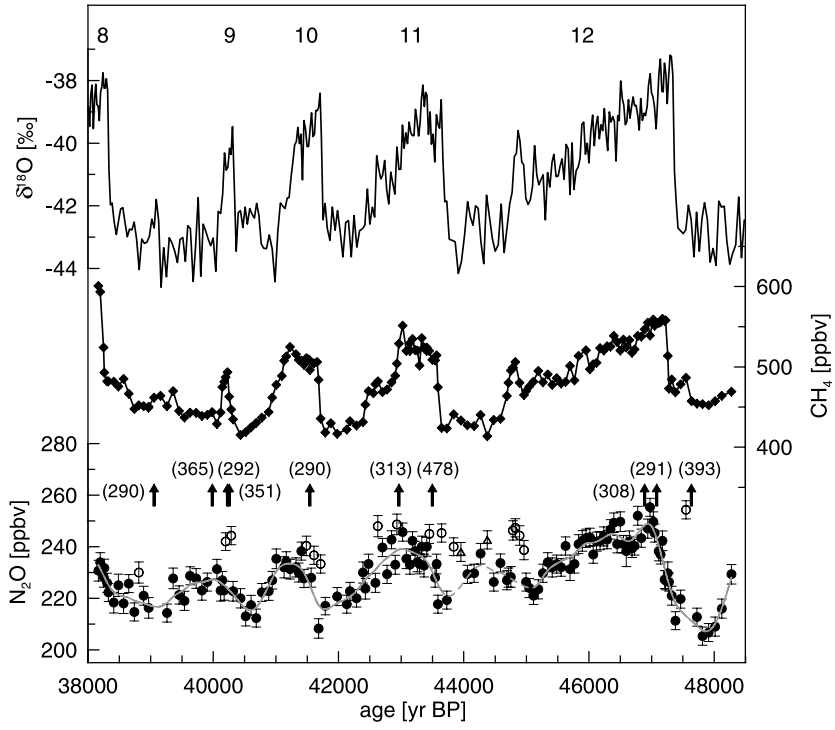

Figure 2. (top) NGRIP $\delta^{18}O$ (S. Johnsen, personal communication, 2003), (middle) CH_4, and (bottom) N_2O record for D-O events 9 to 12. The numbers of the D-O events are indicated in the top part of the figure. For N_2O the 1-sigma uncertainty is given. N_2O data, which are assumed to be artifacts according to the method described in Appendix A, are plotted as open circles. Artifacts that exceed the range of the axes are indicated with arrows at the corresponding age. The values of these artifacts are given in parentheses. In the time period of 43.8 to 44.6 kyr BP, two additional N_2O data points are excluded (open triangles) due to their high sensitivity to changes in the parameters of our method to define artifacts (see Appendix A). To emphasize the atmospheric trend over the whole N_2O data set, a spline with a cutoff period of 600 years is shown (shaded line) [*Enting*, 1987]. The best guess of the possible atmospheric trend in the time period of 43.8 to 45.0 kyr BP is indicated as a shaded dashed line. All data are given on a tentative timescale. The ice age scale is closely related to the GRIP SS09sea timescale [*Johnsen et al.*, 2001]. The gas age scale was calculated from the ice age scale for a temperature scenario of a temperature sensitivity of 0.3‰/°C according to *Schwander et al.* [1997]. These tentative timescales will be improved further in the future. However, our conclusions do not depend on the timescale.

(NGRIP) ice core (75°06′N, 42°20′W) at 158 and 164 different depth levels for N_2O and CH_4, respectively. These data cover the time period of D-O events 9 to 12 (Figure 2). The second data set was measured along the Greenland Ice Core Project (GRIP) ice core (72°34′N, 37°37′W). Ninety-six and 107 samples from different depth levels were measured for N_2O and CH_4, respectively, covering the time period of D-O events 19 and 20 (Figure 3). The two data sets yield excellent resolution. The GRIP record achieves a mean time resolution of 97 years and 77 years for N_2O and CH_4, respectively, reaching a resolution of about 30 years for both records at the beginning of D-O event 19. The resolution of the NGRIP records is about 63 years with highest resolutions of up to 35 years at the beginning of D-O events. Neither data set is corrected for gravitational fractionation, which is small for CH_4 (depletion in the order of 4.1 ± 0.8 ppbv for the GRIP record, 4.5 ± 0.5 ppbv for the NGRIP record) and N_2O (enrichment in the order of 2.0 ± 0.3 ppbv for the GRIP record, 2.2 ± 0.3 ppbv for the NGRIP record). The GRIP and the NGRIP N_2O and CH_4 records are available at http://www.ngdc.noaa.gov/paleo/data.html.

2.2. N_2O Artifacts

[6] The N_2O records from the two ice cores are disturbed by artifacts that episodically show concentrations that are too high. This is similar to what was reported in earlier studies for various ice cores from Greenland and Antarctica [*Flückiger et al.*, 1999; *Sowers*, 2001; *Stauffer et al.*, 2003]. No indications are found that results were biased toward concentrations that are too low. Therefore we assume that artifacts are caused by a production of N_2O in situ and that a depletion of N_2O is unlikely. While very high values caused by artifacts can easily be distinguished from the general trend of the record, it is very difficult to discriminate with certainty all measurements that are biased by a smaller surplus of N_2O. To get an atmospheric N_2O record that can be

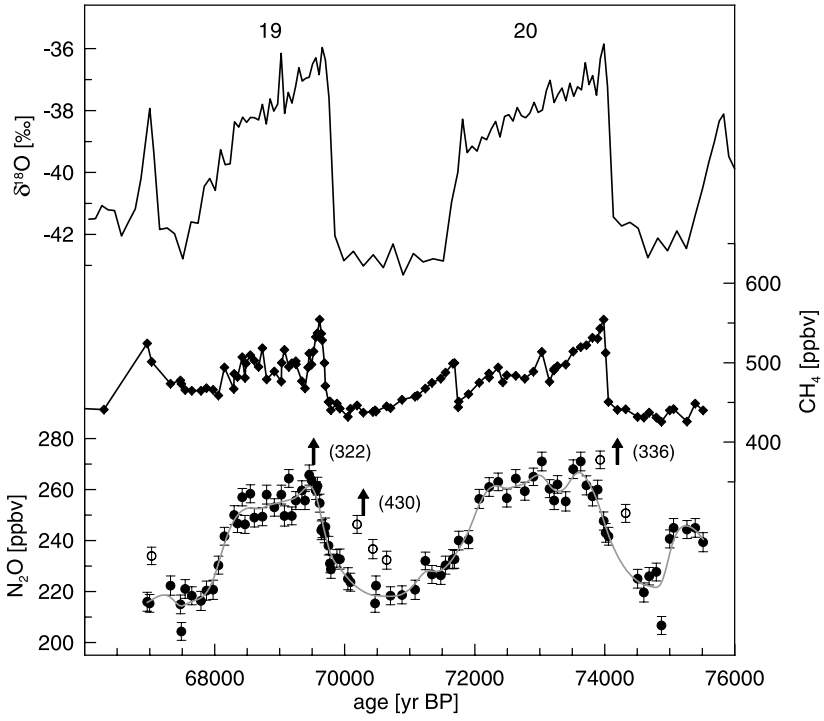

Figure 3. (top) GRIP $\delta^{18}O$ [*Dansgaard et al.*, 1993], (middle) CH_4, and (bottom) N_2O record covering D-O events 19 and 20. For N_2O, the 1-sigma uncertainty is given. N_2O data, which are assumed to be artifacts according to the method described in Appendix A, are plotted as open circles. Artifacts that exceed the range of the axis are indicated with arrows at the corresponding age. The values of these artifacts are given in parentheses. The atmospheric N_2O trend is indicated by the spline with a cutoff period of 600 years (shaded line) [*Enting*, 1987]. All data are shown on the GRIP SS09 timescale [*Johnsen et al.*, 1995; *Schwander et al.*, 1997]. The numbers of the D-O events are indicated in the top part of the figure. The CH_4 and N_2O data presented in this figure as well as in Figure 2 can be downloaded from the World Data Center for Paleoclimatology at Boulder, Colorado (http://www.ngdc.noaa.gov/paleo/data.html).

interpreted in terms of climatic changes, it is crucial to exclude the artifacts from the data sets. The method used is described in Appendix A. Resulting data sets for D-O events 9 to 12 and D-O events 19 and 20 are shown in Figures 2 and 3, respectively. They show the artifacts as well as the remaining record, which is thought to represent the atmospheric variations of the N_2O concentration.

[7] To find the cause of the N_2O artifacts, further investigations were conducted. The surplus of N_2O must be produced in the ice prior to handling and not during the extraction of the air because different extraction techniques yield the same high N_2O outliers [*Kawamura*, 2000; *Sowers*, 2001]. Two mechanisms could lead to the observed surplus of N_2O in distinct depth intervals: chemical reactions and microbiological activity in the ice. Indications for a production by bacteria were previously found in the Vostok ice core in ice from the glacial maximum preceding the Eemian [*Sowers*, 2001]. However, a production by chemical reactions that involves, for example, ammonium (NH_4^-) and nitrate (NO_3^-) cannot be excluded. Less than 1.6% of the present NH_4^- or less than 0.3% of the NO_3^- has to be transformed to N_2O to explain the high N_2O artifacts.

[8] The question arises whether the general trend of the glacial N_2O record is an artifact due to changing concentrations of impurities in the ice. This can be excluded due to the observed depth shift between the climatic signals recorded in the ice (e.g., variations of chemical impurities) and the N_2O concentration recorded in the gas enclosed in the ice (Figure 4). This depth shift accounts for the age difference between ice and enclosed air [*Schwander et al.*, 1997].

[9] Both the NGRIP and GRIP data sets yield artifacts that are mainly located in ice representing transitions from stadials to interstadials and vice versa. To a minor extent, they can be found in ice from cold periods. This is illustrated for the NGRIP measurements in Figure 4. Cold periods are characterized by higher concentrations of dust [*Ruth et al.*, 2003] and chemical impurities, for example, calcium (Ca^{2+}) [*Fuhrer et al.*, 1999], sodium (Na^+), and NO_3^- [*Mayewski et al.*, 1997]. The transitions between stadials and interstadials are marked by changing impurity concentrations and relative compositions of the impurities in the ice. A connection between impurities in the ice and N_2O artifacts is further supported by the fact that no N_2O artifacts were found in ice from the Holocene epoch [*Flückiger et al.*, 2002], which is characterized by much lower impurity

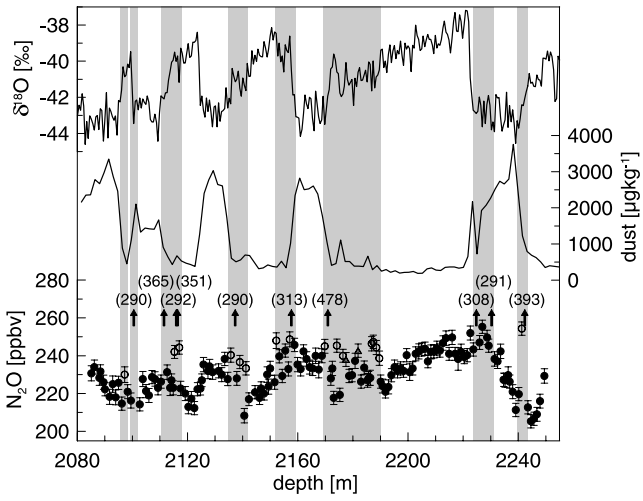

Figure 4. (top) NGRIP $\delta^{18}O$ (S. Johnsen, personal communication, 2003), (middle) dust [*Ruth et al.*, 2003], and (bottom) N_2O covering D-O events 9 to 12 plotted against depth. N_2O artifacts are indicated as in Figure 2. Shaded areas denote depth intervals where artifacts appear in our N_2O data set.

concentrations compared to glacial ice. However, the comparison of surplus N_2O in the NGRIP record and high-resolution chemical records of Ca^{2+}, dust, Na^{+}, NO_3^{-}, and NH_4^{-} measured at the corresponding depths (M. Bigler and R. Röthlisberger, unpublished data, 2003) do not yield a correlation at all [*Flückiger*, 2003]. This indicates that N_2O artifacts do not depend on a single component in the ice but that a combination of different parameters have to be fulfilled for a production of surplus N_2O. Further investigations are needed to understand the causes leading to a production of N_2O in the ice.

3. Results

[10] An overview of the data is given in Figure 1. The N_2O and CH_4 records covering D-O events 9 to 12, and 19 and 20, are shown in detail in Figures 2 and 3, respectively. The CH_4 records compare well with earlier published data sets from Greenland as well as from Antarctica when taking the interpolar difference into account [*Brook et al.*, 1999; *Blunier and Brook*, 2001]. Indeed, the new records unveil variations in much greater detail due to the high time resolution. Previously published N_2O data that overlap partly the records presented in this study are only available for the beginning of D-O event 8 [*Flückiger et al.*, 1999]. Over this time period the NGRIP record is in good agreement with the measurements from Greenland and Antarctica.

[11] The main characteristics of the N_2O records are concentration variations in phase with all investigated D-O events. N_2O increases at the beginning of the D-O events and decreases at the end. No large variations or trends are found during the mild phase of the D-O events except for event 12 where the concentration starts to decrease exceptionally early at about 45,800 years before present (45.8 kyr BP), approximately 1000 years before the main CH_4 decrease at the end of the D-O event. This N_2O decrease is interrupted by an unusual plateau (45 to 44 kyr BP) before the concentration reaches the stadial level between D-O events 12 and 11. The amplitude of the N_2O variations is largest for the long-lasting D-O events 12, 19, and 20. For the shorter D-O events 9, 10, and 11 the N_2O amplitude decreases as the duration of the events decreases.

[12] CH_4 variations associated with D-O events 9 to 12 are characterized by a sharp increase at the beginning and a relatively sharp decrease at the end of the warm events. This observation precludes smoothing of atmospheric variations due to the process of gas trapping as an explanation for the decreasing N_2O amplitudes. The general evolution of the CH_4 concentration during the mild phases differs from event to event with either gradually increasing, decreasing, or stable concentrations, except for D-O events 19 and 20. The CH_4 increase at the beginning of these events is 110 and 120 ppbv, respectively, which is comparable to others, for example, event 12, but these peak concentrations are followed by an unusually fast decrease to much lower values that characterize the main part of the two events.

[13] A detailed comparison of CH_4 with $\delta^{18}O$ illustrates that their general trends during the mild phase of D-O events do not show the same evolution. Even so, in addition to the sharp increases/decreases at the beginning/end of D-O events, some submillennial variations in CH_4 and $\delta^{18}O$ coincide within the dating uncertainty of the gas and the ice age scale during D-O events 9 to 12. Other submillennial changes, however, cannot be found in both records. A decoupling of $\delta^{18}O$ and CH_4 is even more pronounced during D-O events 19 and 20. The comparison of CH_4 and $\delta^{18}O$ could help to determine whether submillennial temperature variations were of local, regional or hemispheric extent and shed light on the possibility that changes of the vapor source regions of the precipitation influenced at least a part of the submillennial changes seen in $\delta^{18}O$.

[14] Important insight into the processes during fast climatic variations and the response of different ecosystems to climatic changes during the last glacial epoch are obtained from the comparison of the N_2O and CH_4 records. We will focus our discussion on two main points. First, the long-term variation of the average amplitudes of the N_2O and CH_4 concentration changes across D-O events will be discussed (section 4.1.). Second, time lags between $\delta^{18}O$, CH_4, and N_2O are observed at the beginning of long-lasting D-O events. The interpretation of these is considered in section 4.2.

4. Discussion

4.1. Response of N_2O and CH_4 to D-O Events on Long-Term Scales

[15] The most pronounced difference between the N_2O and the CH_4 record is the variation in the magnitude of the response of the two greenhouse gases to different D-O events over time. To investigate this different behavior in detail, we calculate the average amplitude for N_2O and CH_4 over the different D-O events in two independent ways. First, we determined the differences between the mean of the stadial levels before and after each individual event and the corresponding averaged interstadial level. Second, for events with a high time resolution, the average amplitude

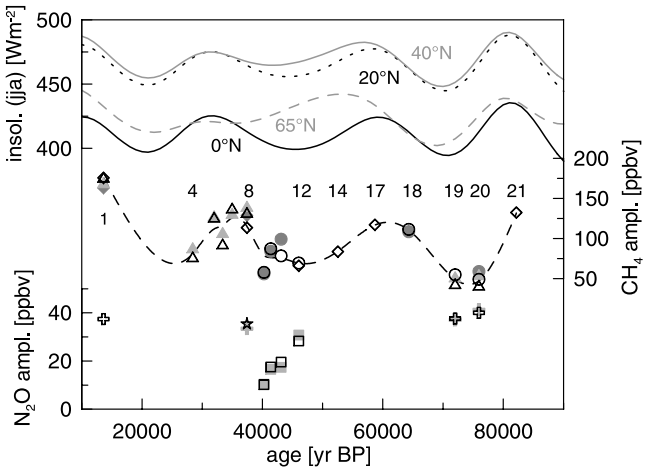

Figure 5. Insolation averaged over the months of June, July, and August at the equator (black solid line), at 20°N (black dotted line), at 40°N (shaded solid line), and at 65°N (shaded dashed line) [*Berger*, 1978] compared to the calculated average amplitudes for GRIP CH_4 (triangles) (*Dällenbach et al.* [2000], *Blunier and Brook* [2001], and this study), NGRIP CH_4 (circles) (this study and J. Chappellaz, unpublished data, 2003), GISP2 CH_4 (diamonds) [*Brook et al.*, 1999; *Blunier and Brook*, 2001], GRIP N_2O (crosses), NGRIP N_2O (squares), and a combination of GRIP, NGRIP, and Byrd N_2O (star) [*Flückiger et al.*, 1999]. Average amplitudes were calculated in two ways: as differences between the average of stadial levels before and after the event and the corresponding average interstadial level (black open symbols) and for events with a higher time resolution additionally as the heights of equilateral trapezoids fitted to the data (shaded solid symbols). To highlight the long-term variation in the average CH_4 amplitude, a spline with a cutoff period of 10 kyr [*Enting*, 1987] (black dashed line) was calculated through the average values of the two different methods. The mean age of the D-O events was deduced from the improved GRIP timescale SS09sea [*Johnsen et al.*, 2001].

was calculated as the height of equilateral trapezoids fitted to the data of each individual D-O event and the stadials before and after the event. The equilateral trapezoids were optimized to the smallest possible squared deviation from the data by adjusting the baseline, the starting time, and the angle of the increase as well as the heights and the length of each individual event. The results of the two methods are in good agreement and show only slight differences for CH_4 as well as for N_2O (Figure 5).

[16] The average amplitudes are thought to be a measure of the average change of the climatic factors that controlled the N_2O and CH_4 concentrations during D-O events. The question arises whether the long-term trends in the average amplitudes correlate with variations in the baselines of the records, which are defined by the different stadial levels. To investigate this for CH_4 the method developed for excluding N_2O artifacts (see Appendix A) was applied to a CH_4 record composed of time-synchronized CH_4 data from GRIP, GISP2 [*Blunier and Brook*, 2001], and NGRIP. For the calculation a cutoff period of 20 kyr and an offset value of 15 ppbv were used. The calculated baseline for the Greenland CH_4 record shows small variations around an average value of 450 ppbv between 77 and 47 kyr BP. The baseline then decreases linearly toward the Last Glacial Maximum (LGM), which shows a mean concentration of 360 ppbv (Figure 1). It is apparent that the variations in this baseline and the average amplitude of CH_4 are not related. Further, the long-term trend in the amplitude is mainly determined by changes in the mean concentration during D-O events rather than changes in the baseline. The same is assumed for N_2O. Owing to the incomplete glacial record of N_2O and the low resolution of the CH_4 record over part of the glacial period, the following discussion focuses only on the average amplitude of the two greenhouse gas variations.

[17] The average amplitude of CH_4 during D-O events in the last glacial epoch shows a strong imprint of the precession cycle of the Milankovitch forcing, similar to that seen for the tropical and mid-northern latitude summer insolation (Figure 5) [*Brook et al.*, 1996]. That implies that the amount or the seasonal distribution of solar radiation influences mechanisms controlling the response of CH_4 to D-O events. The average amplitude of N_2O does not show such a relation. This is, for example, documented in the high N_2O amplitudes for D-O events 19 and 20, which coincide with very small CH_4 amplitudes and small tropical and mid-northern latitude summer insolation. The average amplitude of N_2O rather correlates with the duration of the D-O events (Figure 6).

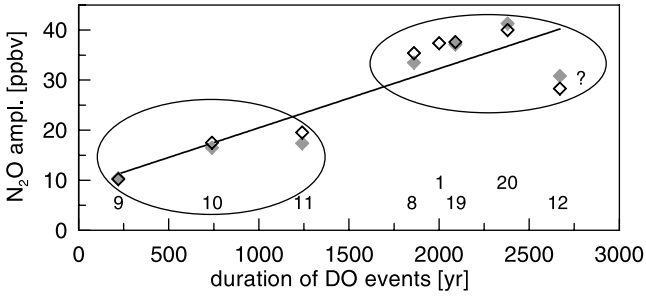

Figure 6. N_2O amplitude versus duration of D-O events. The amplitudes are adopted from Figure 5 (shaded solid symbols: fits of equilateral trapezoids; black open symbols: deduced from mean values of stadial and interstadial levels). Owing to the unusual evolution of the N_2O concentration during D-O event 12, it is difficult to give an accurate value for the N_2O amplitude during this event (indicated by a question mark). The length of the different D-O events was determined by the GRIP $\delta^{18}O$ record on the SS09sea timescale [*Johnsen et al.*, 2001]. The linear relation of the N_2O amplitude to the duration of the D-O events is indicated with the black line representing the linear fit through the average values of the two different methods to determine the amplitude (correlation coefficient $r^2 = 0.77$). Highlighted are further the two groups of D-O events: the long events preceded by a significant warming in the south and the shorter events, which have no significant counterpart in the south. The numbers of the individual D-O events are indicated in the lower part of the figure.

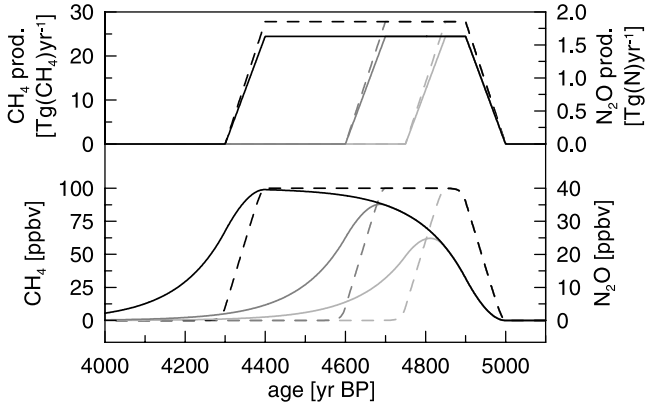

Figure 7. Atmospheric N_2O and CH_4 concentrations calculated for different source evolutions assuming constant lifetimes (N_2O: 120 years, CH_4: 10 years). (top) Total N_2O sources (solid lines, right axis) and CH_4 sources (dashed lines, left axis). The duration of the N_2O and CH_4 source increases and decreases is 100 years. This corresponds roughly to the duration of the CH_4 source increase at the beginning of D-O events. (bottom) Corresponding atmospheric N_2O (solid lines, right axis) and CH_4 concentrations (dashed lines, left axis).

[18] For N_2O the question arises whether the close relation of N_2O amplitude and event duration is due to slowly changing sources, which do not have the time to reach their full interstadial level during short events, and/or the long lifetime of N_2O of 120 years [*Minschwaner et al.*, 1998], which smoothes the atmospheric signal. The latter is only significant for very short D-O events such as D-O event 9. For events that last longer than 500 years, the smoothing due to the long lifetime of N_2O is less than 5% (Figure 7) and, therefore, not the main reason for small N_2O amplitudes. To investigate the response of the total N_2O source to different D-O events the evolution of the total N_2O source was calculated from the measured N_2O data under the assumption of a constant lifetime. The evolution of the calculated total source indicates that the amplitude of the source change during the short D-O events is much smaller than during long D-O events although there would be enough time for the total source to reach high interstadial levels even during short D-O events. This means that the climatic parameters that caused the N_2O source changes evolved differently for D-O events of different durations. The events can be divided into two groups characterized by small and large N_2O amplitudes, respectively (Figure 6). They coincide with two different types of D-O events. Large N_2O amplitudes coincide with long D-O events, which are preceded by a significant warming in the Antarctic [*Stocker*, 1998; *Blunier and Brook*, 2001] (D-O events 8, 12, 19, and 20). Shorter events, which have no significant counterpart in the south, are characterized by lower N_2O amplitudes (D-O events 9, 10, and 11). It is hypothesized that the former follow a state with no North Atlantic deepwater formation and start with a full recovery of the thermohaline circulation, while the latter are preceded by a weak deepwater formation state [*Stocker and Marchal*, 2000; *Ganopolski and Rahmstorf*, 2001]. In the following, we will investigate the different sinks and sources of CH_4 and N_2O and possible mechanisms leading to the different observed long-term trends in the average amplitudes.

4.1.1. CH_4

[19] Three different mechanisms could be responsible for the CH_4 concentration increase during D-O events and variations in the average amplitude of the CH_4 response to D-O events: (1) changes in the CH_4 sink due to changing OH concentrations in the atmosphere; (2) changes in the extent and/or productivity of global wetland areas; and/or (3) releases of CH_4 from methane hydrates in marine sediments.

[20] The main sink for atmospheric CH_4 is its oxidation by OH radicals within the troposphere. Atmospheric chemical models indicate that changes in the sink account only for a small part of the atmospheric CH_4 concentration change during the last glacial-interglacial transition [*Crutzen and Brühl*, 1993; *Thompson et al.*, 1993; *Martinerie et al.*, 1995]. Therefore we focus on the source intensity as an explanation for the CH_4 variations during D-O events.

[21] The main CH_4 sources in pre-anthropogenic times are wetlands [*Chappellaz et al.*, 1993; *Brook et al.*, 1996], which are predominantly located in tropical regions and in the northern extra-tropics. The southern extra-tropics are of minor importance due to the small land surface area in these latitudes [*Walter et al.*, 2001; *Kaplan*, 2002]. CH_4 emissions from wetlands depend mainly on precipitation and temperature with wetter and warmer conditions enhancing emissions [*Matthews*, 2000]. Changes in precipitation patterns and temperature are therefore likely to have caused variations in the extent and productivity of wetland ecosystems.

[22] Although the uncertainty of source distribution calculations from interpolar CH_4 gradients are large, they indicate that the CH_4 increase during D-O events may have its origin mainly in sources located north of 30°N [*Brook et al.*, 1999; *Dällenbach et al.*, 2000]. A higher CH_4 productivity of these wetlands is in principle consistent with the large temperature increases in the north associated with D-O events. The long-term trend in the average amplitude of CH_4, however, cannot be explained by long-term variations in the temperature alone. The temperature in Greenland and probably in the Northern Hemispheric CH_4 source regions increased significantly more at the beginning of D-O event 19 (with a small CH_4 amplitude) than during D-O event 8 (with a large CH_4 amplitude) [*Jouzel*, 1999; *Lang et al.*, 1999]. Possibly a combination of temperature and humidity change can explain the long-term trend in the CH_4 amplitude. This would imply that D-O events with a high temperature increase, like event 19, were relatively dry, leading to a smaller CH_4 production increase than during other events. Changes in the extent of ice sheets, which modulated the ice free area may additionally have contributed to the long-term variation in the CH_4 amplitude [*Brook et al.*, 1996].

[23] Further indications come from the comparison of the long-term variation of the average CH_4 amplitude and the mean insolation of the summer months June, July, and August, which correspond to the important season for CH_4 production in northern latitudes [*Fung et al.*, 1991;

Christensen et al., 2003]. The strong imprint of the precession cycle of the orbital forcing in the CH_4 amplitudes correlates with the summer insolation in mid-northern latitudes, while summer insolation in high northern latitudes is dominated rather by the obliquity cycle (Figure 5). In glacial epochs, wetlands possibly migrated south to mid-northern latitudes where they may have undergone changes in response to the local summer insolation. A strong imprint of the precession cycle can also be found in the tropics, which are the latitudes with the highest CH_4 emissions at present and during the last glacial epoch. This points toward the hypothesis that the tropics are another key region for the variations in the last glacial epoch.

[24] Palaeo-records from tropical and subtropical Asia [*Schulz et al.*, 1998; *Wang et al.*, 2001] and tropical Africa [*Gasse*, 2000; *Stager et al.*, 2002] show variations associated with D-O events. They indicate higher southwest monsoon activity during D-O events than during stadial periods implying enhanced precipitation and CH_4 emissions in these regions during D-O events. The picture of long-term variations in the monsoon intensity is not homogeneous in records from different sites [*Leuschner and Sirocko*, 2000; *Wang et al.*, 2001], but at least some studies [*Clemens et al.*, 1991; *Gasse*, 2000] indicate a correlation to low northern latitude summer insolation and therefore to the variations in the average amplitude of CH_4.

[25] Records from the Amazon show high-frequency variations, which may be related to D-O events [*Maslin and Burns*, 2000; *van der Hammen and Hooghiemstra*, 2003]. On the basis of these records it is assumed that the moisture budget in the Amazon Basin changed in phase with D-O events. Precipitation changes further have a strong imprint of the precession cycle [*Hooghiemstra and van der Hammen*, 1998]. In summary, it is not possible to draw definitive conclusions as to whether changes in the northern extra-tropics or in the tropical regions are mainly responsible for the observed CH_4 oscillations associated with D-O events, as well as for the average CH_4 amplitude changes on long-term scales.

[26] Another hypothesis involves the release of CH_4 from methane hydrates in marine sediments to explain the CH_4 variations in phase with D-O events [*Kennett et al.*, 2003]. However, emissions to the atmosphere via catastrophic events are unlikely given the long durations of D-O events 9 through 12, 19, and 20. The high resolution of the records implies that short-lived (thus catastrophic) events did not occur during these intervals [*Brook et al.*, 2000]. However, we do not exclude the possibility that more regular emissions from CH_4 hydrates may cause a small contribution to the CH_4 variations in phase with the D-O events.

4.1.2. N_2O

[27] Possible causes for concentration fluctuations of N_2O associated with D-O events are terrestrial sources located mainly in the tropics and to a minor extent in temperate regions. Emission rates from soils depend essentially on precipitation and temperature and are therefore closely linked to climatic changes [*Bouwman et al.*, 1993; *Potter et al.*, 1996; *Bollmann and Conrad*, 1998]. Further candidates are changes in the open ocean nitrification [*Nevison et al.*, 1995; *Suntharalingam and Sarmiento*, 2000] and variations in the denitrification in oceanic upwelling areas, for example, in the Arabian Sea and the eastern tropical North Pacific [*Dore et al.*, 1998; *Bange et al.*, 2001]. The main sinks of N_2O are photodissociation (90%) and reactions with excited oxygen (10%) in the stratosphere. Chemical models of the atmosphere have shown that the relative change of the stratospheric N_2O sink is small between the LGM and the preindustrial period [*Crutzen and Brühl*, 1993]. We therefore assume that changes in the N_2O sources of up to 1.6 Tg N yr^{-1} were responsible for the atmospheric concentration variations during the last glacial epoch rather than variations in the destruction processes of N_2O and focus our further discussion on the different sources.

[28] Today's terrestrial N_2O sources in high northern latitudes are small [*Bouwman et al.*, 1993; *Potter et al.*, 1996]. It is assumed that these sources were of even minor importance during glacial times. Temperature and precipitation changes in the moderate northern latitudes and especially in the tropics, however, influence the source strength in these regions and likely have led to enhanced emissions during D-O events.

[29] Other important sources of N_2O are denitrification and nitrification in the ocean. These sources could be partly responsible for the N_2O variations in phase with D-O events and the different response of N_2O and CH_4 to these events on long-term scales.

[30] In general, the denitrification in the world's ocean was strongly reduced during glacial times [*Ganeshram et al.*, 2002] in line with the generally lower atmospheric N_2O concentrations during these time periods. During D-O events, however, important upwelling areas like the Arabian Sea [*Schulz et al.*, 1998; *Suthhof et al.*, 2001] and the eastern tropical North Pacific [*Emmer and Thunell*, 2000; I. L. Hendy et al., The intermittent existence of a southern California upwelling cell during submillennial climate change of the last 60 kyr, submitted to *Paleoceanography*, 2003] (hereinafter referred to as Hendy et al., submitted manuscript, 2003) show high denitrification rates. These are documented on the California margin as close correspondence between sea-surface temperature changes and the $\delta^{15}N$ in bulk sediments (Hendy et al., submitted manuscript, 2003). Warming events, as recorded by lighter values in the $\delta^{18}O$ of planktonic foraminifera, are associated with heavier $\delta^{15}N$ values implying most intense denitrification in sediments deposited on the margin during D-O events. Inferred increases in denitrification in the Arabian Sea during D-O events are very similar. These high denitrification rates have been linked to high export production associated with enhanced upwelling. Both effects are related to episodic shifts in the tropical Pacific Ocean/atmosphere system [*Stott et al.*, 2002].

[31] Denitrification rates in the Arabian Sea during D-O events are believed to be similar to those observed today and low or even zero during stadials. Modern N_2O emissions from the Arabian Sea are 0.21 to 0.50 Tg N yr^{-1} [*Bange et al.*, 2001]. A source change of this magnitude corresponds to a concentration change of 5 to 12 ppbv when assuming a constant lifetime of 120 years [*Minschwaner et al.*, 1998]. Changes in the denitrification rates in the important upwelling regions such as the Arabian Sea and

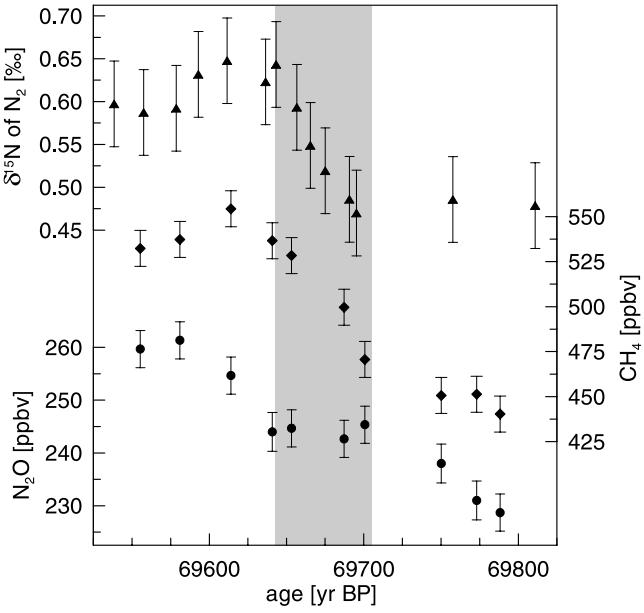

Figure 8. GRIP $\delta^{15}N$ of N_2 (triangles) [*Lang et al.*, 1999], CH_4 (diamonds), and N_2O (circles) at the beginning of D-O event 19. The data are shown together with their 1-sigma uncertainty. The three proxies are all measured on the air enclosed in the ice and can therefore be compared without any relative time uncertainty. The used timescale is GRIP SS09 as in Figure 3. The shaded area denotes the time period of the temperature increase as deduced from the $\delta^{15}N$ record.

the tropical North Pacific could therefore explain a significant part of the atmospheric N_2O variations during D-O events. The most pronounced changes in the extent of denitrification implied by the Arabian Sea $\delta^{15}N$ data are found during the long D-O events. These correspond to the events that have the largest N_2O amplitudes while shorter variations in the Greenland $\delta^{18}O$ record are associated with a much smaller or even negligible change in the marine denitrification record and smaller N_2O amplitudes.

[32] Open-ocean nitrification is dependent on stratification of the upper water masses. Increased stratification leads to decreased upwelling of nutrients into the euphotic zone as well as a physical reduction of N_2O emissions. Model results show that the increased stratification that results from a reduction in deep water formation during the Younger Dryas event indeed probably led to a reduction in the N_2O emissions. Solubility effects due to changing sea surface temperatures and increased storage of N_2O in the ocean were of minor importance [*Goldstein et al.*, 2003]. The same impact of stratification is assumed to have been active during the last glacial epoch, causing smaller N_2O emissions during stadials and higher emissions during interstadials, and thereby contributing to the N_2O concentration changes associated with D-O events.

[33] Knowing the main sources of N_2O, it is likely that a combination of oceanic and terrestrial sources have led to the observed concentration variation during D-O events. This is in line with findings from an isotope study of N_2O covering D-O event 1 during the last glacial-interglacial transition [*Sowers et al.*, 2003].

4.1.3. Comparison of N_2O and CH_4

[34] What causes the different response of N_2O and CH_4 to D-O events over time? Four hypotheses are possible. (1) Changes in the sink of one or both greenhouse gases are responsible for the different response of CH_4 and N_2O to D-O events over time. (2) Contrasts between the two records point to partly different terrestrial source regions, for example, different latitudinal bands, which are responsible for the concentration variations of the two greenhouse gases during D-O events. (3) The terrestrial sources are located in the same regions, but wetlands producing CH_4 are more sensitive to different interstadial levels of precipitation and temperature than the soils producing N_2O. (4) The ocean is the important key player for N_2O.

[35] We exclude the hypothesis that one or both records are dominated by changes in their sinks. In both cases the sinks seem to be of minor importance for the difference in the atmospheric concentration between the LGM and the preindustrial time period [*Crutzen and Brühl*, 1993; *Thompson et al.*, 1993; *Martinerie et al.*, 1995]. It can therefore be assumed that the influence was also small during climatic variations of the last glacial period. Still, we note that such a conclusion remains based on very few modeling experiments that were applied to glacial conditions and were based on major assumptions on, for example, the fluxes of other trace species (nitrogen oxides, carbon monoxide, ozone) and the troposphere/stratosphere exchange which are still unconstrained at that point.

[36] N_2O and CH_4 both have important soil sources. Does the different response to D-O events over time support the hypothesis that different regions, for example, different latitudinal bands were responsible for the concentration fluctuations associated with D-O events? This is not compelling, because different soil conditions favor N_2O or CH_4 emissions. While CH_4 is produced in soils with 100% water saturation, the production of N_2O has its optimum at 60 to 90% water-filled pore space in the soil and ceases as the water-filled pore space approaches 100% [*Davidson*, 1991]. CH_4 could therefore be more sensitive to changes in moisture content in the soil due to changing temperature and precipitation than N_2O. Such a situation is indicated for the first part of the Holocene. The evolution of N_2O does not follow the drying in the tropics as reported in the CH_4 record [*Flückiger et al.*, 2002], implying that the terrestrial N_2O sources in the tropics were probably not affected in the same way as the wetlands. Temperature and precipitation changes in phase with D-O events thus could lead to changes in the terrestrial N_2O and CH_4 sources in the same region but with a higher sensitivity of CH_4 to the interstadial moisture status. Therefore it cannot a priori be excluded that the causes for the two different long-term trends in the response to D-O events are located in the same latitudes. Nevertheless, we cannot exclude differences in the latitudinal distribution of the terrestrial N_2O and CH_4 sources responsible for the concentration variations. While the changing terrestrial

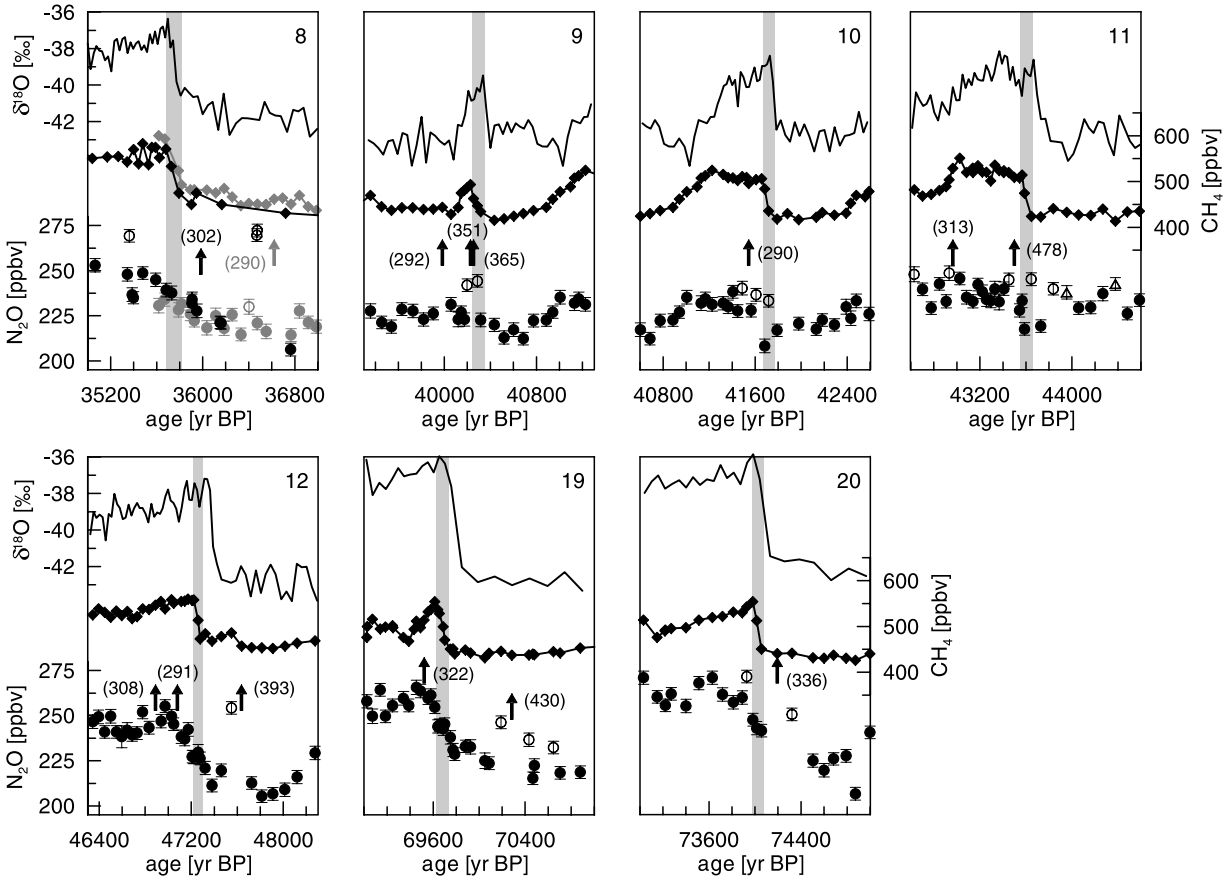

Figure 9. Details of the beginnings of D-O events 8 to 12, 19, and 20. For each individual D-O event, $\delta^{18}O$ (top traces), CH_4 (middle traces), and N_2O (bottom traces) are shown as in Figures 2 and 3. The corresponding number of the D-O event is marked in each window. Data for D-O events 9 to 12 are from NGRIP. They are plotted on the tentative NGRIP timescale. The records for D-O events 19 and 20 are from the GRIP core on the GRIP SS09 timescale. For D-O event 8, GRIP data (black) are shown together with the NGRIP CH_4 and N_2O records (shaded). The used timescale for this event is the GRIP SS09 timescale. The NGRIP data of D-O event 8 were matched to the GRIP data using the CH_4 records of the two cores. The shaded areas denote the time period of the CH_4 increases. The $\delta^{18}O$ values are only shown for orientation. Owing to the uncertainty in the difference between the gas and the ice age scale, the precise timing of the $\delta^{18}O$ increases and the greenhouse gas concentration changes cannot be deduced from this figure. CH_4 and N_2O, however, can be compared without any relative time uncertainty because both components are measured on the air enclosed in the same ice.

source of N_2O is located in tropical and subtropical regions, the tropical and high northern latitudes could be both responsible for the CH_4 variations.

[37] An unlikely hypothesis is that the terrestrial sources of N_2O did not show oscillations associated with D-O events and the N_2O concentration predominantly reflects changing oceanic sources. The CH_4 variations document that soils underwent dramatic shifts in the production due to temperature and precipitation changes. These climatic changes certainly influenced the N_2O production in soils as well. Therefore a combination of terrestrial and oceanic sources is more likely responsible for the N_2O variations during the last glacial epoch. Oceanic sources, however, could be responsible for the contrast in the N_2O amplitudes of D-O events of different duration. Support for this hypothesis is provided by the fact that CH_4, which is probably mainly a terrestrial product, shows no such pattern.

4.2. Start of Dansgaard-Oeschger Events

[38] The high-resolution N_2O and CH_4 measurements performed on the same samples offer the opportunity to compare the two records without any relative time uncertainty, whereas the comparison with the $\delta^{18}O$ record measured along the same core is only possible within the uncertainty of delta age, i.e., the time difference between the ice and the enclosed air [*Schwander et al.*, 1997]. Additional information about the timing of the temperature increase recorded in Greenland ice cores and the CH_4 record at the beginning of D-O events comes from measurements of $\delta^{15}N$ of N_2 in the bubbles enclosed in the ice, which is

another proxy for temperature. For the transitions from the late glacial epoch to the Bølling-Allerød and from the Younger Dryas to the Holocene, it was found that the start of the CH_4 increase lags the beginning of the temperature increase by 0 to 30 years, and that the increase lasts several decades longer than the temperature increase [*Severinghaus et al.*, 1998; *Severinghaus and Brook*, 1999]. The comparison of $\delta^{15}N$ [*Lang et al.*, 1999] and CH_4 measurements performed on the GRIP core excludes a lag of CH_4 to $\delta^{15}N$ at the beginning of D-O event 19. Rather, the data suggest that the beginning of the CH_4 increase was synchronous with the start of the warming (Figure 8). As for the other events, the CH_4 increase lasts several decades longer than the temperature increase revealed in the $\delta^{15}N$ record. According to these results, we assume that the CH_4 increase at the beginning of D-O events is synchronous with the temperature increase, within a few decades.

[39] The comparison of N_2O to CH_4 shows that two types of events must be distinguished (Figure 9). During the long D-O events (8, 12, 19, and 20) the N_2O concentration starts to increase continuously several hundred years before the main CH_4 rise, and thus also leads the beginning of the sharp temperature increase reconstructed for Greenland. For the shorter D-O events presented in this study the data are less clear. However, they indicate that within the resolution of the data, and, at least for D-O events 10 and 11, the start of the N_2O increase did not precede but was rather synchronous with the beginning of the CH_4 rise.

[40] The long D-O events (8, 12, 19, and 20) are preceded by a significant slow warming in Antarctica, which starts about 1500 to 3000 years before the sharp temperature increase of the corresponding D-O events observed in the north [*Blunier and Brook*, 2001]. A similar warming has been found for at least part of the Southern Hemisphere outside Antarctica [*Voelker and Workshop Participants*, 2002], for example, for the Southern Ocean surface temperature [*Charles et al.*, 1996; *Ninnemann et al.*, 1999] and in the South Atlantic [*Vidal et al.*, 1999], and has also been suggested by models [*Stocker*, 1998; *Vellinga and Wood*, 2002]. A close relation between the early N_2O rise and the warming in the south can be excluded due to the very different timing of the two records. The N_2O concentration starts to increase more than 1000 years later than the southern warming in all the cases.

[41] It is further known that D-O events 8 and 12 are preceded by massive iceberg discharges, Heinrich events H4 and H5, respectively [*Hemming*, 2004]. In MIS 4, for example, before D-O events 19 and 20, distinct events are missing in the deep-sea records [*Hemming*, 2004]. A direct link of the early increase of N_2O to Heinrich events can therefore be excluded.

[42] The missing link of the early rise of N_2O to known climatic changes indicates that a picture of North Atlantic instability causing the D-O events may be too simple. Instead, it points to changes in other parts of the Earth's climate system that start before the abrupt warming event recorded in Greenland. Such changes could be an early warming in the tropics, or early shifts in some parts of the ocean, that cause the ocean to approach the threshold where deepwater formation through convection abruptly starts. Early changes are, for example, seen in the intermediate waters of the Santa Barbara basin [*Hendy and Kennett*, 2003]. Finding the cause of the early start of the rise in N_2O concentration is a crucial task for future research, because it will certainly yield further insight into complex global processes that are associated with climatic variations on millennial time scales in glacial epochs and could give insight into a precursor of D-O events.

[43] Although N_2O starts to rise earlier than CH_4, at least at the beginning of long D-O events, the concentration increase lasts significantly longer than for CH_4. While the main increases of CH_4 at the beginning of the D-O events discussed here are completed within less than 150 years, interstadial levels of N_2O are reached 200 to 400 years later. This longer-lasting increase can mainly be explained by the longer lifetime of N_2O (120 years [*Minschwaner et al.*, 1998], versus 10 years for CH_4 [*Martinerie et al.*, 1995; *Chappellaz et al.*, 1997]) (Figure 7).

5. Conclusion

[44] CH_4 and N_2O both show concentration variations in phase with D-O events in the last glacial epoch. However, significant differences exist in their response to D-O events over time. While the average amplitude of CH_4 shows a close relation to the precession component of tropical and mid-northern latitude summer insolation, N_2O amplitudes correlate instead with the duration of the D-O events. The arrangement of the D-O events into two groups of large and small N_2O amplitudes supports the view of two types of D-O events with different extent and, perhaps, different underlying process. The long-lasting D-O events are preceded by a significant warming in the south and have larger N_2O amplitudes than the shorter events with no significant southern-warming counterparts. Further, models suggest that the long events follow an ocean state without North Atlantic deep water formation, while the shorter events are associated with only a shift and amplification of the deepwater formation [*Stocker and Marchal*, 2000; *Ganopolski and Rahmstorf*, 2001]. For the longer D-O events, N_2O starts to increase several hundred years before the main CH_4 and temperature increases recorded in Greenland but more than 1000 years after the beginning of the warming in Antarctica. This indicates that changes related to D-O events in some parts of the climate system preceded the abrupt warming observed in Greenland.

[45] Additional work is necessary if the assessment and attribution of gas sources is to be improved for individual events. In particular, emphasis needs to be placed on a better reconstruction and understanding of precipitation and temperature variations in different latitudes and their associated impacts on terrestrial CH_4 and N_2O sources. Furthermore, there is an obvious need to gain more insight into the oceanic N_2O source and its variation in the last glacial period. In addition to the understanding that can be gained by terrestrial and oceanic models, through which the different responses of CH_4 and N_2O sources to climatic changes in the past can be investigated, additional high-resolution ice core data should provide insight into the responsible mechanisms. For example, CH_4 gradient and source-distri-

bution calculations provide a powerful means to probe the changing response of CH_4 sources to different D-O events. However, this is not an option for N_2O due to the small interhemispheric gradient (only about 0.8 ppbv today [*IPCC*, 2001]). Improved attribution of sources of CH_4 and N_2O can also be expected from measurements of their isotopic composition and from the intramolecular site preference in N_2O isotopomers. In addition a better understanding of fractionation processes and the isotopic signature associated with each individual source is required especially for N_2O to reduce uncertainties in isotope calculations.

Appendix A: Method to Exclude N_2O Artifacts

[46] A smoothed spline is calculated through the full N_2O data set. Data points with a positive offset of more than a certain value (hereinafter referred to as the "offset value") to the spline are considered as artifacts and are excluded from the record. This procedure is applied iteratively until none of the individual points in the data set exceeds the spline by more than the offset value. The important parameters to be determined are the offset value and the degree of smoothing by the spline function. The offset value is set to 8 ppbv, which is on the order of the mean 2-sigma uncertainty of each individual data point. The smoothing of the spline function excludes all periods lower than a certain cutoff period [*Enting*, 1987]. To estimate the cutoff period to be applied to the data set, a suite of variations of the total N_2O source that have a triangular or a trapezoidal shape is simulated, resulting in atmospheric variations of 14 to 49 ppbv. The spline method is then applied to the individual signals adjusting the cutoff period to the highest value where none of the data points are excluded. The simulations start from a steady state situation with a source of 0 Tg N yr^{-1}. The source is then increased in the range of 2.04 Tg N yr^{-1} to 2.85 Tg N yr^{-1} in 1 to 50 years. This is equivalent to 50 to 70 ppbv at steady state, corresponding to the largest increase observed at the beginning of a D-O event and the glacial-interglacial transition, respectively. The source is then decreased at a rate of 0.005 Tg N yr^{-2}, which roughly corresponds to the fastest concentration decrease in the record at the end of D-O event 19. Further, to exclude an underestimation, a decrease is simulated at a rate of 0.02 Tg N yr^{-2}. The duration of the entire source perturbation is varied from 100 to 600 years. The range of calculated cutoff periods from these simulations is 400 to 750 years. To exclude artifacts from the GRIP and NGRIP N_2O data sets, a cutoff period of 600 years is used, which is within this range. The choice of this cutoff period is supported by the lack of overshooting of the spline in any part of the GRIP and the NGRIP record. Furthermore, small variations in the data sets as a result of the measurement uncertainty are cancelled out while variations related to D-O events are still nicely reported in the spline. Small changes in the offset parameter and the cutoff period do not have a significant influence on the N_2O data sets except from the depth interval of 2176 to 2184 m in the NGRIP core (about 43.8 to 44.6 kyr BP). In this interval, the determination of artifacts is very sensitive to small changes in the timescale and the cutoff period. Two additional data points in this depth interval are excluded and are highlighted in the figures. This shows the limitation of the used artifact identification algorithm in depth intervals with a little bit lower time resolution and a scattering of the data, which is slightly higher than on average. However, all the conclusions of the paper do not depend on individual data points and are therefore not sensitive to small changes in the two parameters of our artifact identification method.

[47] **Acknowledgments.** We thank T. F. Pedersen and R. Knutti for fruitful discussions and helpful comments on the manuscript. Comments of two anonymous reviewers further improved the paper. This work, as part of the NorthGRIP project, was supported by the University of Bern and the Swiss National Science Foundation. The NorthGRIP project is directed and organized by the Department of Geophysics at the Niels Bohr Institute for Astronomy, Physics and Geophysics, University of Copenhagen. It is being supported by Funding Agencies in Denmark (SNF), Belgium (FNRS-CFB), France (IFRTP and INSU/CNRS), Germany (AWI), Iceland (RannIs), Japan (MEXT), Sweden (SPRS), Switzerland (SNF), and the United States of America (NSF). Partial support through contract EVK2-2000-22067 (POP) by the Swiss Federal Office of Science and Education is acknowledged.

References

Bange, H. W., M. O. Andreae, S. Lal, C. S. Law, S. W. A. Naqvi, P. K. Patra, T. Rixen, and R. C. Upstill-Goddard (2001), Nitrous oxide emissions from the Arabian Sea: A synthesis, *Atmos. Chem. Phys.*, *1*, 61–71.

Berger, A. (1978), Long-term variations of daily insolation and Quaternary climatic changes, *J. Atmos. Sci.*, *35*(12), 2362–2367.

Blunier, T., and E. Brook (2001), Timing of millennial-scale climate change in Antarctica and Greenland during the last glacial period, *Science*, *291*, 109–112.

Bollmann, A., and R. Conrad (1998), Influence of O_2 availability on NO and N_2O release by nitrification and denitrification in soils, *Global Change Biol.*, *4*, 387–396.

Bouwman, A. F., I. Fung, E. Matthews, and J. John (1993), Global analysis of the potential for N_2O production in natural soils, *Global Biogeochem. Cycles*, *7*(3), 557–597.

Brook, E. J., T. Sowers, and J. Orchardo (1996), Rapid variations in atmospheric methane concentration during the past 110,000 years, *Science*, *273*, 1087–1091.

Brook, E. J., S. Harder, J. Severinghaus, and M. Bender (1999), Atmospheric methane and millennial-scale climate change, in *Mechanisms of Global Climate Change at Millennial Time Scale*, *Geophys. Monogr. Ser.*, vol. 112, edited by P. U. Clark, R. S. Webb, and L. D. Keigwin, pp. 165–175, AGU, Washington, D. C.

Brook, E. J., S. Harder, J. Severinghaus, E. J. Steig, and C. M. Sucher (2000), On the origin and timing of rapid changes in atmospheric methane during the last glacial period, *Global Biogeochem. Cycles*, *14*(2), 559–572.

Chappellaz, J., T. Blunier, D. Raynaud, J. M. Barnola, J. Schwander, and B. Stauffer (1993), Synchronous changes in atmospheric CH_4 and Greenland climate between 40 and 8 kyr BP, *Nature*, *366*, 443–445.

Chappellaz, J., T. Blunier, S. Kints, A. Dällenbach, J.-M. Barnola, J. Schwander, D. Raynaud, and B. Stauffer (1997), Changes in the atmospheric CH_4 gradient between Greenland and Antarctica during the Holocene, *J. Geophys. Res.*, *102*(D13), 15,987–15,999.

Charles, C. D., J. Lynch-Stieglitz, U. S. Ninnemann, and R. G. Fairbanks (1996), Climate connections between the hemispheres revealed by deep sea sediment core/ice core correlations, *Earth Planet. Sci. Lett.*, *142*, 19–27.

Christensen, T. R., A. Ekberg, L. Ström, M. Mastepanov, M. Öquist, B. H. Svensson, H. Nykänen, P. J. Martikainen, and H. Oskarsson (2003), Factors controlling large scale variations in methane emissions from wetlands, *Geophys. Res Lett.*, *30*(7), 1414, doi:10.1029/2002GL016848.

Clemens, S., W. Prell, D. Murray, G. Shimmield, and G. Weedon (1991), Forcing mechanisms of the Indian Ocean monsoon, *Nature*, *353*, 720–725.

Crutzen, P. J., and C. Brühl (1993), A model study of atmospheric temperatures and the concentration of ozone, hydroxyl, and some other photochemical active gases during the glacial, the preindustrial Holocene and the present, *Geophys. Res Lett.*, *20*(11), 1047–1050.

Dällenbach, A., B. Blunier, J. Flückiger, B. Stauffer, J. Chappellaz, and D. Raynaud (2000), Changes in the atmospheric CH_4 gradient between Greenland and Antarctica during the last glacial and the transition to the Holocene, *Geophys. Res. Lett.*, *27*(7), 1005–1008.

Dansgaard, W., et al. (1993), Evidence for general instability of past climate from a 250 kyr ice-core record, *Nature*, *364*, 218–220.

Davidson, E. A. (1991), Fluxes of nitrous oxide and nitric oxide from terrestrial ecosystems, in *Microbial Production and Consumption of Greenhouse Gases: Methane, Nitrogen Oxides and Halomethanes*, edited by J. E. Rogers and W. B. Whitman, pp. 219–235, Am. Soc. for Microbiol., Washington, D. C.

Dore, J. E., B. N. Popp, D. M. Karl, and F. J. Sansone (1998), A large source of atmospheric nitrous oxide from subtropical North Pacific surface waters, *Nature*, *396*, 63–66.

Emmer, E., and R. C. Thunell (2000), Nitrogen isotope variations in Santa Barbara Basin sediments: Implications for denitrification in the eastern tropical North Pacific during the last 50,000 years, *Paleoceanography*, *15*(4), 377–387.

Enting, I. G. (1987), On the use of smoothing splines to filter CO_2 data, *J. Geophys. Res.*, *92*(D9), 10,977–10,984.

Flückiger, J. (2003), Nitrous oxide and methane variations covering the last 100,000 years: Insight into climatic and environmental processes, Ph.D. thesis, 116 pp., Phys. Inst., Univ. of Bern, Bern.

Flückiger, J., A. Dällenbach, T. Blunier, B. Stauffer, T. F. Stocker, D. Raynaud, and J.-M. Barnola (1999), Variations in atmospheric N_2O concentration during abrupt climatic changes, *Science*, *285*, 227–230.

Flückiger, J., E. Monnin, B. Stauffer, J. Schwander, T. F. Stocker, J. Chappellaz, D. Raynaud, and J.-M. Barnola (2002), High resolution Holocene N_2O ice core record and its relationship with CH_4 and CO_2, *Global Biogeochem. Cycles*, *16*(1), 1010, doi:10.1029/2001GB001417.

Fuhrer, K., E. W. Wolff, and S. J. Johnsen (1999), Timescales for dust variability in the Greenland Ice Core Project (GRIP) ice core in the last 100,000 years, *J. Geophys. Res.*, *104*(D24), 31,043–31,052.

Fung, I., J. John, J. Lerner, E. Matthews, M. Prather, L. P. Steele, and P. J. Fraser (1991), Three-dimensional model synthesis of the global methane cycle, *J. Geophys. Res.*, *96*(D7), 13,033–13,065.

Ganeshram, R. S., T. F. Pedersen, S. E. Calvert, and R. François (2002), Reduced nitrogen fixation in the glacial ocean inferred from changes in marine nitrogen and phosphorus inventories, *Nature*, *415*, 156–159.

Ganopolski, A., and S. Rahmstorf (2001), Rapid changes of glacial climate simulated in a coupled climate model, *Nature*, *409*, 153–158.

Gasse, F. (2000), Hydrological changes in the African tropics since the last glacial maximum, *Quat. Sci. Rev.*, *19*, 189–211.

Goldstein, B., F. Joos, and T. F. Stocker (2003), A modeling study of oceanic nitrous oxide during the Younger Dryas cold period, *Geophys. Res Lett.*, *30*(2), 1092, doi:10.1029/2002GL016418.

Hemming, S. R. (2004), Heinrich events: Massive late Pleistocene detritus layers of the North Atlantic and their global climate imprint, *Rev. Geophys.*, doi:10.1029/2003RG000128, in press.

Hendy, I. L., and J. P. Kennett (2003), Tropical forcing of North Pacific intermediate water distribution during Late Quaternary rapid climate change?, *Quat. Sci. Rev.*, *22*, 673–689.

Hooghiemstra, H., and T. van der Hammen (1998), Neogene and quaternary development of the neotropical rain forest: The forest refugia hypothesis, and a literature overview, *Earth Sci. Rev.*, *44*, 147–183.

Indermühle, A., E. Monnin, B. Stauffer, T. F. Stocker, and M. Wahlen (2000), Atmospheric CO_2 concentration from 60 to 20 kyr BP from the Taylor Dome ice core, Antarctica, *Geophys. Res. Lett.*, *27*(5), 735–738.

Intergovernmental Panel on Climate Change (2001), *Climate Change 2001: The Scientific Basis, Contribution of Working Group I to the Third Assessment Report of the Intergovernmental Panel on Climate Change*, edited by J. T. Houghton et al., 881 pp., Cambridge Univ. Press, New York.

Johnsen, S. J., W. Dansgaard, H. B. Clausen, and C. C. Langway Jr. (1972), Oxygen isotope profiles through the Antarctic and Greenland ice sheets, *Nature*, *235*, 429–434.

Johnsen, S. J., D. Dahl-Jensen, W. Dansgaard, and N. Gundestrup (1995), Greenland paleotemperatures derived from GRIP bore hole temperature and ice core isotope profiles, *Tellus, Ser. B*, *47*, 624–629.

Johnsen, S. J., D. Dahl-Jensen, N. Gundestrup, J. P. Steffensen, H. B. Clausen, H. Miller, V. Masson-Delmotte, A. E. Sveinbjörnsdottir, and J. White (2001), Oxygen isotope and palaeotemperature records from six Greenland ice-core stations: Camp Century, Dye 3, GRIP, GISP2, Renland and NorthGRIP, *J. Quat. Sci.*, *16*(4), 299–307.

Jouzel, J. (1999), Calibrating the isotopic paleothermometer, *Science*, *286*, 910–911.

Kaplan, J. O. (2002), Wetlands at the Last Glacial Maximum: Distribution and methane emissions, *Geophys. Res Lett.*, *29*(6), 1076, doi:1029/2001GL013366.

Kawamura, K. (2000), Variations of atmospheric components over the past 340,000 years from Dome Fuji deep ice core, Antarctica, Ph.D. thesis, 212 pp., Tohoku Univ., Tohoku.

Keeling, C. D., and T. P. Whorf (2000), Atmospheric CO_2 records from sites in the SIO air sampling network, in *Trends: A Compendium of Data on Global Change*, Carbon Dioxide Inf. Anal. Cent., Oak Ridge Natl. Lab., U.S. Dep. of Energy, Oak Ridge, Tenn.

Kennett, J. P., K. G. Cannariato, I. L. Hendy, and R. J. Behl (2003), *Methane Hydrates in Quaternary Climate Change: The Clathrate Gun Hypothesis*, *Spec. Publ.*, vol. 54, 216 pp., AGU, Washington, D. C.

Lang, C., M. Leuenberger, J. Schwander, and S. Johnsen (1999), 16°C rapid temperature variation in central Greenland 70,000 years ago, *Science*, *286*, 934–937.

Leuschner, D. C., and F. Sirocko (2000), The low-latitude monsoon climate during Dansgaard-Oeschger cycles and Heinrich events, *Quat. Sci. Rev.*, *19*, 243–254.

Martinerie, P., G. P. Brasseur, and C. Granier (1995), The chemical composition of ancient atmospheres: A model study constrained by ice core data, *J. Geophys. Res.*, *100*(D7), 14,291–14,304.

Maslin, A. M., and S. J. Burns (2000), Reconstruction of the Amazon basin effective moisture availability over the past 14,000 years, *Science*, *290*, 2285–2287.

Matthews, E. (2000), Wetlands, in *Atmospheric Methane: Its Role in the Global Environment*, edited by M. A. K. Khalil, pp. 202–233, Springer-Verlag, New York.

Mayewski, P. A., L. D. Meeker, M. S. Twickler, S. Whitlow, Q. Yang, W. B. Lyons, and M. Prentice (1997), Major features and forcing of high-latitude Northern Hemisphere atmospheric circulation using a 110,000-year-long glaciochemical series, *J. Geophys. Res.*, *102*(C12), 26,345–26,366.

Minschwaner, K., R. W. Carver, B. P. Briegleb, and A. E. Roche (1998), Infrared radiative forcing and atmospheric lifetimes of trace species based on observations from UAES, *J. Geophys. Res.*, *103*(D18), 23,243–23,253.

Nevison, C. D., R. F. Wiess, and D. J. Erickson (1995), Global oceanic emission of nitrous oxide, *J. Geophys. Res.*, *100*(C8), 15,809–15,820.

Ninnemann, U. S., C. D. Charles, and D. A. Hodell (1999), Origin of global millennial scale climate events: Constraints from the Southern Ocean deep sea sedimentary record, in *Mechanism of Global Climate Change at Millennial Time Scales*, *Geophys. Monogr. Ser.*, vol. 112, edited by P. U. Clark, R. S. Webb, and L. D. Keigwin, pp. 99–112, AGU, Washington, D. C.

Petit, J. R., et al. (1999), Climate and atmospheric history of the past 420,000 years from the Vostok ice core, Antarctica, *Nature*, *399*, 429–436.

Potter, C. S., P. A. Matson, P. M. Vitousek, and E. A. Davidson (1996), Process modeling of controls on nitrogen trace gas emissions from soils worldwide, *J. Geophys. Res.*, *101*(D1), 1361–1377.

Ruth, U., D. Wagenbach, J. P. Steffensen, and M. Bigler (2003), Continuous record of microparticle concentration and size distribution in the central Greenland NGRIP ice core during the last glacial period, *J. Geophys. Res.*, *108*(D3), 4098, doi:10.1029/2002JD002376.

Schulz, H., S. von Rad, and H. Erlenkeuser (1998), Correlation between Arabian Sea and Greenland climate oscillations of the past 110,000 years, *Nature*, *393*, 54–57.

Schwander, J., T. Sowers, J.-M. Barnola, T. Blunier, B. Malaizé, and T. Fuchs (1997), Age scale of the air in the summit ice: Implication for glacial-interglacial temperature change, *J. Geophys. Res.*, *102*(D16), 19,483–19,494.

Severinghaus, J. P., and E. J. Brook (1999), Abrupt climate change at the end of the last glacial period inferred from trapped air in polar ice, *Science*, *286*, 930–934.

Severinghaus, J. P., T. Sowers, E. J. Brook, R. B. Alley, and M. L. Bender (1998), Timing of abrupt climate change at the end of the Younger Dryas interval from thermally fractionated gases in polar ice, *Nature*, *391*, 141–146.

Sowers, T. (2001), The N_2O record spanning the penultimate deglaciation from the Vostok ice core, *J. Geophys. Res.*, *106*(D23), 31,903–31,914.

Sowers, T., R. B. Alley, and J. Jubenville (2003), Ice core records of atmospheric N_2O covering the last 106,000 years, *Science*, *301*, 945–948.

Stager, J. C., P. A. Mayewski, and L. D. Meeker (2002), Cooling cycles, Heinrich event 1, and the desiccation of Lake Victoria, *Palaeogeogr. Palaeoclimatol. Palaeoecol.*, *183*, 169–178.

Stauffer, B., J. Flückiger, E. Monnin, J. Schwander, J.-M. Barnola, and J. Chappellaz (2002), Atmospheric CO_2, CH_4 and N_2O records over the past 60,000 years based on the comparison of different polar ice cores, *Ann. Glaciol.*, *35*, 202–208.

Stauffer, B., J. Flückiger, E. Monnin, T. Nakazawa, and S. Aoki (2003), Discussion of the reliability of CO_2, CH_4 and N_2O records from polar ice cores, in *Global Scale Climate and Environment Study Through Polar Deep Ice Cores*, edited by H. Shoji and O. Watanabe, pp. 139–152, Natl. Inst. of Polar Res., Tokyo.

Stocker, T. F. (1998), The seesaw effect, *Science*, *282*, 61–62.

Stocker, T. F., and O. Marchal (2000), Abrupt climate change in the coomputer: Is it real?, *Proc. U.S. Natl. Acad. Sci.*, *97*(4), 1362–1365.

Stott, L., C. Poulsen, S. Lund, and R. Thunell (2002), Super ENSO and global climate oscillation at millennial time scale, *Science*, *297*, 222–226.

Suntharalingam, P., and J. L. Sarmiento (2000), Factors governing the oceanic nitrous oxide distribution: Simulations with an ocean general circulation model, *Global Biogeochem. Cycles*, *14*(1), 429–454.

Suthhof, A., V. Ittekkot, and B. Gaye-Haake (2001), Millennial-scale oscillation of denitrification intensity in the Arabian Sea during the late Quaternary and its potential influence on atmospheric N_2O and global climate, *Global Biogeochem. Cycles*, *15*(3), 637–649.

Thompson, A. M., J. A. Chappellaz, I. Y. Fung, and T. L. Kucsera (1993), The atmospheric CH_4 increase since the Last Glacial Maximum: 2. Interactions with oxidants, *Tellus, Ser. B*, *45*, 242–257.

van der Hammen, T., and H. Hooghiemstra (2003), Interglacial-glacial Fuquene-3 pollen record from Colombia: An Eemian to Holocene climate record, *Global Planet. Change*, *36*(3), 181–199.

Vellinga, M., and R. A. Wood (2002), Global climatic impacts of a collapse of the Atlantic thermohaline circulation, *Clim. Change*, *54*, 251–267.

Vidal, L., R. R. Schneider, O. Marchal, T. Bickert, T. F. Stocker, and G. Wefer (1999), Link between the North and South Atlantic during the Heinrich events of the last glacial period, *Clim. Dyn.*, *15*, 909–919.

Voelker, A. H. L. (2002), Global distribution of centennial-scale records for Marine Isotope Stage (MIS) 3: A database, *Quat. Sci. Rev.*, *21*, 1185–1212.

Walter, B. P., M. Heimann, and E. Matthews (2001), Modeling modern methane emissions from natural wetlands: 1. Model description and results, *J. Geophys. Res.*, *106*(D24), 34,189–34,206.

Wang, Y. J., H. Cheng, R. L. Edwards, Z. S. An, J. Y. Wu, C.-C. Shen, and J. A. Dorale (2001), A high-resolution absolute-dated late Pleistocene monsoon record from Hulu Cave, China, *Science*, *294*, 2345–2348.

T. Blunier, J. Flückiger (corresponding author), K. Kawamura, J. Schwander, R. Spahni, B. Stauffer, and T. F. Stocker, Climate and Environmental Physics, Physics Institute, University of Bern, Sidlerstrasse 5, 3012 Bern, Switzerland. (blunier@climate.unibe.ch; flueckiger@climate.unibe.ch; kawamura@climate.unibe.ch; schwander@climate.unibe.ch; spahni@climate.unibe.ch; stauffer@climate.unibe.ch; stocker@climate.unibe.ch)

J. Chappellaz, CNRS Laboratoire de Glaciologie et Géophysique de l'Environnement (LGGE), Boîte Postale 96, 38402 St. Martin d'Hères Cedex, Grenoble, France. (jerome@lgge.obs.ujf-grenoble.fr)

D. Dahl-Jensen, Niels Bohr Institute, Department of Geophysics, University of Copenhagen, Juliane Maries Vej 30, 2100 Copenhagen, Denmark. (ddj@gfy.ku.dk)